MITSUBISHI ELECTRIC RESEARCH LABORATORIES
http://www.merl.com

Range Accuracy Analysis for FMCW Systems with Source Nonlinearity

Wang, P.; Millar, D.S.; Parsons, K.; Ma, R.; Orlik, P.V.

TR2019-018 April 24, 2019

Abstract

In this paper, we provide theoretical analysis on range estimation in frequency modulated continuous wave (FMCW) systems when the source nonlinearity is present. Existing literature on the effect of source nonlinearity on the range estimation is either based on a heuristic approach or limited to specific algorithms. To provide a unified analysis, we introduce the framework of misspecified Cramér-Rao bound (MCRB) and derive analytical lower bounds on the range estimation. Our analysis reveals that the range estimation accuracy is a function of the nonlinearity function, system parameters (e.g., bandwidth, sampling frequency) and noise variance. It is also noted that our result converges to the conventional accuracy analysis for range estimation when the nonlinearity becomes negligible. Finally, numerical results are provided to verify the analytical bounds.

IEEE International Conference on Microwaves for Intelligent Mobility (ICMIM 2019)

Range Accuracy Analysis for FMCW Systems with Source Nonlinearity

Pu Wang, David Millar, Kieran Parsons, Rui Ma, Phillip V. Orlik

***Abstract*— In this paper, we provide theoretical analysis on range estimation in frequency modulated continuous wave (FMCW) systems when the source nonlinearity is present. Existing literature on the effect of source nonlinearity on the range estimation is either based on a heuristic approach or limited to specific algorithms. To provide a unified analysis, we introduce the framework of misspecified Cramér-Rao bound (MCRB) and derive analytical lower bounds on the range estimation. Our analysis reveals that the range estimation accuracy is a function of the nonlinearity function, system parameters (e.g., bandwidth, sampling frequency) and noise variance. It is also noted that our result converges to the conventional accuracy analysis for range estimation when the nonlinearity becomes negligible. Finally, numerical results are provided to verify the analytical bounds.**

***Index Terms*— Range estimation, source nonlinearity, frequency modulated continuous wave, Cramér-Rao bound.**

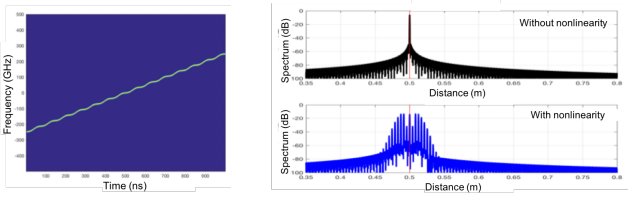

(a) linearly swept source with sinusoidal source nonlinearity in the time-frequency domain.

(b) Range Estimation without (top) and with (bottom) sinusoidal source nonlinearity.

Fig. 1. The impact of a sinusoidal source nonlinearity on FMCW-based range estimation in the optical frequency range.

I. Introduction

Linearly swept or frequency modulated continuous wave (FMCW) sources in the radio and optical frequency ranges have been used to estimate the distance of reflectors with high resolution, low hardware cost, and lightweight signal processing. FMCW radar, optical frequency-domain reflectometry (OFDR) and swept-source optical coherence tomography (SS-OCT) are typical applications of linear sweep sources.

An FMCW system transmits linearly frequency-modulated continuous waves, whose frequency pattern follows a sawtooth or triangular pattern with respect to time [1]–[3]. Reflected signals from various objects of interest are mixed with the local oscillator signal, which is used to generate the transmitted signal, to produce analog beat signals and output digital beat signals via analog-to-digital converters (ADCs). Since the peak frequency of beat signal is proportional to the distance of object, a standard fast Fourier transform (FFT) of the beat signal can be used to identify peaks and, hence, estimate the distance.

One of key issues for the FMCW system is that, as shown in Fig. 1, range resolution and estimation accuracy degrade when the source is not linearly swept [4]–[9]. The source nonlinearity can be caused by phase noise at local oscillators, low-cost voltage controlled oscillator (VCO), imprecise frequency tracking, switching in digital circuits, and the transient response of the phase-locked loop (PLL) component. Moreover, the nonlinearity effect on the range estimation is range-dependent, smaller at short measurement distances and greater at long measurement distances. For short-distance targets, it is possible to compensate the nonlinearity in the beat signal directly using the original nonlinearity at the source. For long-distance targets, on the other hand, the nonlinearity effect aggravates along with target distance, leading to a primary disturbance source.

The nonlinearity can be compensated with *hardware* and *software* solutions. Hardware solutions include the use of a predistorted VCO control voltage to have a linear FM output and complex synthesizer with phase-locked loop. However, the former approach fails when the external conditions, e.g., temperature, are changing, while the latter requires costly devices. The use of direct digital synthesis (DDS) offers effective solutions, but the transmitted bandwidth is still limited when compared to the one obtained by directly sweeping the VCO [10]. Different local oscillators can be used to transmit large bandwidths at the cost of increased system complexity.

On the other hand, software solutions mostly use a reference point to estimate the source nonlinearity function [1], [3], [9], [11]–[14]. With the estimated nonlinearity function, the nonlinearity effect is compensated with respect to the beat signal to restore the correct phase information. These computational methods include resampling of the data in order to have a linear behavior and matched filtering with a function estimated from the reference response. However, these approaches are based on local approximations of the source nonlinearity function, which limits their applicability to short-range applications. [1] and [2] presented a nonlinearity correction algorithm which removes the nonlinearity effects over the entire range profile. The method is based on the residual-video-phase (RVP) correction and operates on the de-ramped data. When the source nonlinearity is time-varying due to external operating conditions, e.g., temperature, vibration, and electromagnetic noise, reference-based approaches have to repeat the step of estimating the source nonlinearity function and update it in the nonlinearity correction method [14]. [9] presented a parametric reference-free approach to jointly estimate range parameters of multiple reflectors and the source nonlinearity function from the beat signal. Given a parametric (e.g., sinusoidal or polynomial) model for the nonlinearity function, the beat signal can be shown to be the sum of K responses characterized by K reflectors and a shared set of parametric coefficients for the nonlinearity function. Therefore, by jointly estimating the two sets of unknown parameters from the K-component beat signal, the range information can be recovered. It is noted that this reference-free approach requires the number of reflectors to be above a threshold that is determined by the parametric model used for the source nonlinearity.

In practice, the source nonlinearity is often ignored due to the high cost of hardware solutions and increased computational complexity of software solutions. Therefore, there is considerable interest to understand the performance loss when source nonlinearity is present [15]–[18]. [15] characterized the nonlinearity effect due to the phase

The authors are with Mitsubishi Electric Research Laboratories (MERL), 201 Broadway, Cambridge, MA 02139, USA (e-mail: {pwang, millar, parsons, rma, porlik}@merl.com).

noise at local oscillators and its contribution to the intermediate frequency (IF) spectrum by modeling the phase noise as a stochastic process. [10] used a simple definition of nonlinearity of a W-band FMCW sensor as the ratio of change in the frequency slope to the slope. The resulting range resolution is defined as the root mean square of the conventional range resolution and the product between the nonlinearity term and target range. As the nonlinearity term increases or the range is increased, the range resolution becomes worse and hence target resolving capability is reduced. [16] focused on analyzing the effects of systematic nonlinearities on bias and variance of the Fourier transform-based target range estimates. [17] extended similar analysis to cooperative radar systems. In [18], the FMCW nonlinearity was measured and then characterized as the combination of 1) random deviation due to phase noise and 2) periodic (sinusoidal) deviations due to switching in digital circuits or transient response of the PLL component. Given such nonlinearity characterization, the standard CRB framework was used to analyze the dependence of target range estimation accuracy on the frequency ramp nonlinearity, phase noise, and SNR.

In this paper, we provide a unified analysis on FMCW-based range estimation when the source nonlinearity is present. Compared with previous studies that are either based on a heuristic approach or limited to specific algorithms, we introduce the framework of *misspecified* Cramér-Rao bound (MCRB) and derive analytical lower bounds on the FMCW-based range estimation directly as an explicit function of source nonlinearity, system parameters (e.g., bandwidth, sampling frequency) and SNR. It is also noted that our result converges to the conventional accuracy analysis for FMCW-based range estimation when the nonlinearity becomes negligible. Finally, numerical results are provided to verify the analytical bounds.

The remainder of this paper is organized as follows. Section II introduces the FMCW-based range estimation and the effect of source nonlinearity. The misspecified CRB is derived in details in Section III. Numerical examples are provided in Section IV to verify the analytical result, followed by a conclusion in Section V.

II. Nonlinearity-Induced Range Distortion in FMCW Systems

Consider an FMCW system transmitting a unit-magnitude linearly frequency modulated signal

$$s_t(t) = e^{j2\pi(f_c t + 0.5\alpha t^2 + \epsilon(t))}, \tag{1}$$

where t is the time variable, f_c is the carrier frequency, α is the frequency sweep rate or chirp rate, and $\epsilon(t)$ is the source nonlinearity phase function. For a perfect FMCW source, we have $\epsilon(t) = 0$.

For a stationary reflector at a distance of R, the received signal is a delayed and attenuated copy of the transmitted signal

$$\begin{aligned} s_r(t) &= Ae^{j\phi_0} s_t(t-\tau) \\ &= Ae^{j\phi_0} e^{j2\pi(f_c(t-\tau)+0.5\alpha(t-\tau)^2+\epsilon(t-\tau))}, \end{aligned} \tag{2}$$

where $Ae^{j\phi_0}$ is the complex amplitude reflected from the target and $\tau = 2R/c$ is the time delay. It is then mixed with the transmitted signal to generate the beat signal.

$$\begin{aligned} s_b(t) &= s_r(t)s_t^*(t) \\ &= Ae^{j\phi_0} e^{j2\pi(-f_c\tau+\alpha\tau t-0.5\alpha\tau^2+(\epsilon(t)-\epsilon(t-\tau)))}. \end{aligned} \tag{3}$$

With a perfect FMCW source, $\epsilon(t)-\epsilon(t-\tau) = 0$ in (3) and the beat signal is a complex sinusoidal signal with $f_b = \alpha\tau$ (or, equivalently, angular frequency $\omega_b = 2\pi\alpha\tau$). When the source nonlinearity $\epsilon(t)$ is present, the beat signal in (3) is no longer a single-tone signal due to the time-dependent term $\epsilon(t)-\epsilon(t-\tau) \neq 0$ in the phase. As a result, the spectral peak of beat signal can be shifted and spread, resulting in degradation in the range resolution and estimation accuracy. Fig.1 (a) shows the time-frequency spectrum of the linearly swept source signal contaminated by a sinusoidal source nonlinearity due to switching in digital circuits or transient response of the PLL component. Its impact on the range estimation is clearly seen in Fig.1 (b) as the spectrum peak spreads with multiple spurious peaks.

III. Range Accuracy Analysis In The Presence of FMCW Source Nonlinearity

In the following, we characterize performance degradation due to the presence of FMCW source nonlinearity by the means of the misspecified CRB [19]–[23]. To be specific, our goal is, for a given source nonlinearity, to derive the range estimation accuracy as a function of the source nonlinearity and other parameters such as the bandwidth, sampling frequency and the SNR.

To be precise, the noisy beat signal $x_n = s_b(n) + v(n)$ follows a complex Gaussian probability density function (pdf),

$$p_x(x_n) = \mathcal{CN}(\bar{\mu}_n, \bar{\sigma}^2), \tag{4}$$

where the mean is given by the noise-free beat signal in (3)

$$\begin{aligned} \bar{\mu}_n &= s_b(n) = s_b(t)|_{t=n\Delta T} \\ &= Ae^{j2\pi(\alpha\tau n\Delta T+\bar{\phi}_0+(\epsilon(n\Delta T)-\epsilon(n\Delta T-\tau))} \\ &= Ae^{j2\pi(\bar{f}_0 n+\bar{\phi}_0+(\epsilon(n\Delta T)-\epsilon(n\Delta T-\tau))} \end{aligned} \tag{5}$$

where $\bar{f}_0 = \alpha\tau\Delta T$, $\bar{\phi}_0 = f_c\tau - 0.5\alpha\tau^2 + \phi_0$, $\epsilon(n) \neq 0$, and the noise variance is $\bar{\sigma}^2$. Here we use $[\bar{\cdot}]$ to denote the true parameters in the true signal model.

Due to computational complexity and hardware constraints, the FMCW system often ignores the presence of the source nonlinearity $\epsilon(t)$ and simply treats the observed beat signal as if the source nonlinearity term is zero, i.e., $\epsilon(t) = 0$, thus yielding a misspecified signal model, $\mathcal{F}$,

$$f_x(x_n|\boldsymbol{\theta}) = \mathcal{CN}(\mu_n(\boldsymbol{\psi}), \sigma^2), \tag{6}$$

where $\mu_n = Ae^{j2\pi(f_0 n+\phi_0)}$ is the ideal discrete-time beat signal with $\epsilon(t) = 0$. The corresponding parameters in the assumed signal model are grouped as $\boldsymbol{\theta} = [\boldsymbol{\psi}^T, \sigma^2]^T$ with $\boldsymbol{\psi} = [f_0, \phi_0, A]$.

The FMCW-based range estimation is to estimate the signal parameters $\boldsymbol{\psi}$ (particularly f_0 which is directly related to the range) and the noise variance σ^2 according to (6) from observed beat signal actually generated from (4). The problem of interest here is to fully characterize the range estimation accuracy given the model mismatch between (4) and (6). For this purpose, we introduce below the misspecified CRB for analyzing accuracy of FMCW-based range estimation in the presence of source nonlinearity.

A. Pseudo-True Parameter

To derive the misspecified CRB, we need to first find a *unique* set of pseudo-true parameters for $\boldsymbol{\psi}$ and σ^2 in the assumed signal model of (6) which has the smallest Kullback-Leibler divergence (KLD) with respect to the true signal model of (4). The pseudo-true parameter set represents a surrogate parameter set in the assumed signal model of (6). The distance between the true and pseudo-true parameters contributes the range estimation error due to the model mismatch.

Given (4) and (6), the KLD between the two signal models is given as

$$\begin{aligned} D(p_x\|f_x) &= \int \ln\left(\frac{p_x(\mathbf{x})}{f_x(\mathbf{x}|\boldsymbol{\theta})}\right) p_x(\mathbf{x})d\mathbf{x} \\ &= N\ln\frac{\sigma^2}{\bar{\sigma}^2} - N + N\frac{\bar{\sigma}^2}{\sigma^2} + \frac{\|\boldsymbol{\mu}(\boldsymbol{\psi}) - \bar{\boldsymbol{\mu}}\|^2}{\sigma^2} \end{aligned} \tag{7}$$

Given the true $\bar{\boldsymbol{\mu}}$ and $\bar{\sigma}^2$, we can first minimize the KLD over the nonlinear parameter set $\boldsymbol{\psi}$, equivalent to minimizing $\|\boldsymbol{\mu}(\boldsymbol{\psi}) - \bar{\boldsymbol{\mu}}\|^2$, i.e.,

$$\begin{aligned}\boldsymbol{\psi}_0 = [f_0, \phi_0, A_0]^T &= \arg\min_{\boldsymbol{\psi}} \|\bar{\boldsymbol{\mu}} - \boldsymbol{\mu}(\boldsymbol{\psi})\|^2 \\ &= \arg\min_{\boldsymbol{\psi}} \sum_{n=0}^{N-1} \left|\bar{\mu}_n - Ae^{j2\pi(f_0 n+\phi_0)}\right|^2\end{aligned} \tag{8}$$

which can be solved by a nonlinear least squared method or a noiseless phase unwrapping method. With $\boldsymbol{\psi}_0$ and define $|\mu_0|^2 = \|\bar{\boldsymbol{\mu}} - \boldsymbol{\mu}(\boldsymbol{\psi}_0)\|^2/N$, we can minimize the KLD over σ^2 as

$$\sigma_0^2 = \bar{\sigma}^2 + |\mu_0|^2. \tag{9}$$

In other words, in (8), the pseudo-true signal parameters $\boldsymbol{\psi}_0$ minimize the total distance over the two means $\bar{\mu}_n$ and $\mu_n(\boldsymbol{\psi})$. In (9), the pseudo-true nuisance parameter σ_0^2 is found to be the sum of the true noise variance $\bar{\sigma}^2$ and the squared residual term $|\mu_0|^2$.

Grouping the pseudo-true parameter set as $\boldsymbol{\theta}_0 = [\boldsymbol{\psi}_0^T, \sigma_0^2]^T$, we can define the difference vector as $\mathbf{r} = \bar{\boldsymbol{\theta}} - \boldsymbol{\theta}_0$, where $\bar{\boldsymbol{\theta}} = [\bar{f}_0, \bar{\phi}_0, \bar{A}, \bar{\sigma}^2]^T$ is the true parameter set in (4).

B. Misspecified CRB

For any unbiased estimator $\hat{\boldsymbol{\theta}}(\mathbf{x})$, i.e., $\mathbb{E}_p\{\hat{\boldsymbol{\theta}}(\mathbf{x})\} = \boldsymbol{\theta}_0$ (unbiased with respect to the pseudo-true parameters $\boldsymbol{\theta}_0$), then the error covariance matrix of the mismatched estimator is given as

$$\mathbf{C}_p(\hat{\boldsymbol{\theta}}(\mathbf{x}), \boldsymbol{\theta}_0) = \mathbb{E}_p\left\{(\hat{\boldsymbol{\theta}}(\mathbf{x}) - \boldsymbol{\theta}_0)(\hat{\boldsymbol{\theta}}(\mathbf{x}) - \boldsymbol{\theta}_0)^T\right\} \tag{10}$$

where $\boldsymbol{\theta}_0$ is the pseudo-true parameter (defined above), is lower bounded by the misspecified CRB [22]

$$\mathbf{C}_p(\hat{\boldsymbol{\theta}}(\mathbf{x}), \boldsymbol{\theta}_0) \succeq \mathbf{A}_{\boldsymbol{\theta}_0}^{-1}\mathbf{B}_{\boldsymbol{\theta}_0}\mathbf{A}_{\boldsymbol{\theta}_0}^{-1} = \text{MCRB}(\boldsymbol{\theta}_0) \tag{11}$$

where $\mathbf{A}_{\boldsymbol{\theta}_0}$ and $\mathbf{B}_{\boldsymbol{\theta}_0}$ are two generalization of the conventional FIM in the matched signal model case. Specifically, $\mathbf{A}_{\boldsymbol{\theta}_0}$ and $\mathbf{B}_{\boldsymbol{\theta}_0}$ are, respectively, defined as

$$[\mathbf{A}_{\boldsymbol{\theta}_0}]_{ij} = \mathbb{E}_p\left\{\frac{\partial^2 \ln f_x(\mathbf{x}|\boldsymbol{\theta})}{\partial\boldsymbol{\theta}_i\partial\boldsymbol{\theta}_j}|_{\boldsymbol{\theta}=\boldsymbol{\theta}_0}\right\}, \tag{12}$$

with elements obtained by taking the expectation of the second partial derivatives of the *assumed* log-likelihood function $\ln f_x(\mathbf{x}|\boldsymbol{\theta})$ of (6) over the *true* pdf $p_x(\mathbf{x})$ of (4), and

$$[\mathbf{B}_{\boldsymbol{\theta}_0}]_{ij} = \mathbb{E}_p\left\{\frac{\partial \ln f_x(\mathbf{x}|\boldsymbol{\theta})}{\partial\boldsymbol{\theta}_i}|_{\boldsymbol{\theta}=\boldsymbol{\theta}_0}\frac{\partial \ln f_x(\mathbf{x}|\boldsymbol{\theta})}{\partial\boldsymbol{\theta}_j}|_{\boldsymbol{\theta}=\boldsymbol{\theta}_0}\right\}, \tag{13}$$

with elements obtained by taking the expectation of the cross product of first partial derivatives of the *assumed* log-likelihood function $\ln f_x(\mathbf{x}|\boldsymbol{\theta})$ over the *true* pdf $p_x(\mathbf{x})$. In the matched signal model case, we have $\mathbf{A}_{\boldsymbol{\theta}_0} = -\mathbf{B}_{\boldsymbol{\theta}_0}$.

1) Log-Likelihood Function and Its Derivatives: From (6), the assumed log-likelihood function is given as

$$\ln f_x(\mathbf{x}|\boldsymbol{\theta}) = -N\ln\sigma^2 - \frac{\|\mathbf{x} - \boldsymbol{\mu}(\boldsymbol{\psi})\|^2}{\sigma^2}. \tag{14}$$

which leads to $\mu_n = Ae^{j2\pi(f_0 n+\phi_0)}$

$$\frac{\partial \ln f_x(\mathbf{x}|\boldsymbol{\theta})}{\partial f_0} = 2\sigma^{-2}\Re\left\{\mathbf{x}^H\frac{\partial\boldsymbol{\mu}}{\partial f_0}\right\} = \frac{4\pi}{\sigma^2}\Re\left\{j\mathbf{x}^H(\boldsymbol{\mu}\odot\mathbf{n})\right\} \tag{15}$$

$$\frac{\partial \ln f_x(\mathbf{x}|\boldsymbol{\theta})}{\partial \phi_0} = 2\sigma^{-2}\Re\left\{\mathbf{x}^H\frac{\partial\boldsymbol{\mu}}{\partial \phi_0}\right\} = \frac{4\pi}{\sigma^2}\Re\left\{j\mathbf{x}^H\boldsymbol{\mu}\right\} \tag{16}$$

$$\begin{aligned}\frac{\partial \ln f_x(\mathbf{x}|\boldsymbol{\theta})}{\partial A} &= 2\sigma^{-2}\Re\left\{\mathbf{x}^H\frac{\partial\boldsymbol{\mu}}{\partial A}\right\} - 2\sigma^{-2}NA \\ &= \frac{2}{\sigma^2 A}\Re\left\{\mathbf{x}^H\boldsymbol{\mu}\right\} - 2\sigma^{-2}NA\end{aligned} \tag{17}$$

$$\frac{\partial \ln f_x(\mathbf{x}|\boldsymbol{\theta})}{\partial \sigma^2} = -N\sigma^{-2} + \sigma^{-4}\|\mathbf{x} - \boldsymbol{\mu}(\boldsymbol{\psi})\|^2 \tag{18}$$

2) The Generalized FIM $\mathbf{A}_{\boldsymbol{\theta}_0}$ and $\mathbf{B}_{\boldsymbol{\theta}_0}$: The matrix $\mathbf{A}_{\boldsymbol{\theta}_0}$ is obtained by taking the expectation of the second partial derivatives of the *assumed* log-likelihood function $\ln f_x(\mathbf{x}|\boldsymbol{\theta})$ of (6) over the *true* pdf $p_x(\mathbf{x})$ of (4). Plugging (14) into (12) yields

$$\begin{aligned}
\mathbf{A}_{f_0,f_0} &= -\frac{8\pi^2}{\sigma_0^2}\Re\left\{\bar{\boldsymbol{\mu}}^H(\boldsymbol{\mu}\odot\mathbf{n}\odot\mathbf{n})\right\} = -\frac{8\pi^2}{\sigma_0^2}\sum_n n^2\zeta_\Re(n) \\
\mathbf{A}_{\phi_0,\phi_0} &= -\frac{8\pi^2}{\sigma_0^2}\Re\left\{\bar{\boldsymbol{\mu}}^H\boldsymbol{\mu}\right\} = -\frac{8\pi^2}{\sigma_0^2}\sum_n \zeta_\Re(n) \\
\mathbf{A}_{A,A} &= -2N\sigma_0^{-2}, \quad \mathbf{A}_{\sigma^2,\sigma^2} = -N\sigma_0^{-4} \\
\mathbf{A}_{f_0,\phi_0} &= -\frac{8\pi^2}{\sigma_0^2}\Re\left\{\bar{\boldsymbol{\mu}}^H(\boldsymbol{\mu}\odot\mathbf{n})\right\} = -\frac{8\pi^2}{\sigma_0^2}\sum_n n\zeta_\Re(n) \\
\mathbf{A}_{f_0,A} &= \frac{4\pi}{\sigma_0^2 A}\Re\left\{j\bar{\boldsymbol{\mu}}^H(\boldsymbol{\mu}\odot\mathbf{n})\right\} = -\frac{4\pi}{\sigma_0^2 A}\sum_n n\zeta_\Im(n) \\
\mathbf{A}_{f_0,\sigma^2} &= -\frac{4\pi}{\sigma_0^4}\Re\left\{j\bar{\boldsymbol{\mu}}^H(\boldsymbol{\mu}\odot\mathbf{n})\right\} = \frac{4\pi}{\sigma_0^4}\sum_n n\zeta_\Im(n) \\
\mathbf{A}_{\phi_0,A} &= \frac{4\pi}{\sigma_0^2 A}\Re\left\{j\bar{\boldsymbol{\mu}}^H\boldsymbol{\mu}\right\} = -\frac{4\pi}{\sigma_0^2 A}\sum_n \zeta_\Im(n) \\
\mathbf{A}_{\phi_0,\sigma^2} &= -\frac{4\pi}{\sigma_0^4}\Re\left\{j\mathbf{x}^H\boldsymbol{\mu}\right\} = \frac{4\pi}{\sigma_0^4}\sum_n \zeta_\Im(n) \\
\mathbf{A}_{A,\sigma^2} &= -\frac{2}{A_0\sigma_0^4}\sum_n \eta_\Re(n) + 2\sigma_0^{-4}NA_0,
\end{aligned}$$

where $\zeta_\Re(n) = \Re\{\bar{\mu}^*(n)\mu_0(n)\}$ and $\zeta_\Im(n) = \Im\{\bar{\mu}^*(n)\mu_0(n)\}$ are the real and imaginary parts of the n-th component of $\bar{\boldsymbol{\mu}}^*\odot\boldsymbol{\mu}_0$.

Next, the other generalization of the FIM is the matrix $\mathbf{B}_{\boldsymbol{\theta}_0}$ of (13) whose elements are obtained by taking the expectation of the cross product of first partial derivatives of the *assumed* log-likelihood function $\ln f_x(\mathbf{x}|\boldsymbol{\theta})$ over the *true* pdf $p_x(\mathbf{x})$. Plugging (14) into (13) yields

$$\begin{aligned}
\mathbf{B}_{f_0,f_0} &= \frac{8\pi^2\bar{\sigma}^2A_0^2}{\sigma_0^4}\sum_n n^2 + \frac{16\pi^4}{\sigma_0^4}\left(\sum_n n\zeta_\Im(n)\right)^2 \\
\mathbf{B}_{\phi_0,\phi_0} &= \frac{8\pi^2\bar{\sigma}^2A_0^2N}{\sigma_0^4} + \frac{16\pi^2}{\sigma_0^4}\left(\sum_n \zeta_\Im(n)\right)^2 \\
\mathbf{B}_{A,A} &= \frac{4}{\sigma_0^4A_0^2}\left(NA_0^2 - \sum_n \zeta_\Re(n)\right)^2 + \frac{2N\bar{\sigma}^2}{\sigma_0^4} \\
\mathbf{B}_{\sigma^2,\sigma^2} &= \frac{N\bar{\sigma}^2(2\sigma_0^2 - \bar{\sigma}^2)}{\sigma_0^8} \\
\mathbf{B}_{f_0,\phi_0} &= \frac{8\pi^2\bar{\sigma}^2A_0^2}{\sigma_0^4}\sum_n n + \frac{16\pi^2}{\sigma_0^4}\left(\sum_n n\zeta_\Im(n)\right)\left(\sum_n \zeta_\Im(n)\right) \\
\mathbf{B}_{f_0,A} &= \frac{8\pi}{\sigma_0^4A_0}\left(\sum_n n\zeta_\Im(n)\right)\left(NA_0^2 - \sum_n \zeta_\Re(n)\right) \\
\mathbf{B}_{f_0,\sigma^2} &= -\frac{4\pi\bar{\sigma}^2}{\sigma_0^6}\left(\sum_n n\zeta_\Im(n)\right) \\
\mathbf{B}_{\phi_0,A} &= \frac{8\pi}{\sigma_0^4A_0}\left(\sum_n \zeta_\Im(n)\right)\left(NA_0^2 - \sum_n \zeta_\Re(n)\right) \\
\mathbf{B}_{\phi_0,\sigma^2} &= -\frac{4\pi\bar{\sigma}^2}{\sigma_0^6}\left(\sum_n \zeta_\Im(n)\right) \\
\mathbf{B}_{A,\sigma^2} &= -\frac{2\bar{\sigma}^2}{\sigma_0^6A_0}\left(NA_0^2 - \sum_n \zeta_\Re(n)\right).
\end{aligned}$$

3) Convergence to the conventional FIM: If there is no model mismatch and the assumed signal model is the true signal model, i.e., $\bar{\mu}(n) = \mu_0(n)$ and $\bar{\sigma}^2 = \sigma_0^2$, and notice that $\zeta_\Re(n) = A^2$ and

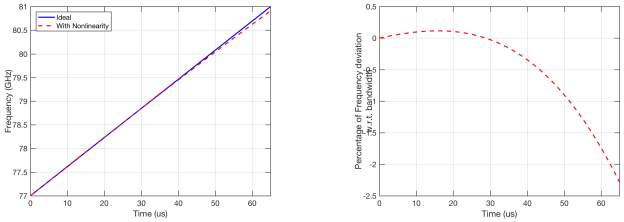

(a) An FMCW spectra

(b) Frequency deviation as a function of bandwidth

Fig. 2. The time-frequency pattern of the FMCW source (a) and frequency deviation as a function of bandwidth (b).

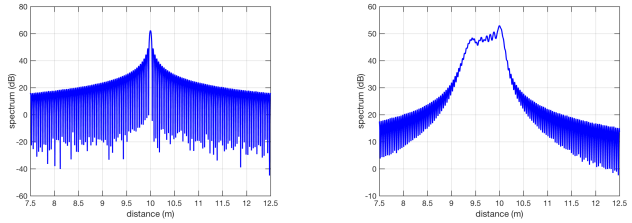

(a) Range spectrum without source nonlinearity

(b) Range spectrum with source nonlinearity

Fig. 3. The effect of source nonlinearity of a 79-GHz FMCW system.

$\zeta_{\Im}(n) = 0$, the above misspecified FIMs $\mathbf{A}_{\boldsymbol{\theta}_0}$ and $\mathbf{B}_{\boldsymbol{\theta}_0}$ reduce to the conventional ones

$$-\mathbf{A}_{\boldsymbol{\theta}_0} = \mathbf{B}_{\boldsymbol{\theta}_0} = \mathbf{I} = \begin{bmatrix} \frac{8\pi^2 A_0^2 \sum_n n^2}{\sigma_0^2} & \frac{8\pi^2 A_0^2 \sum_n n}{\sigma_0^2} & 0 & 0 \\ \frac{8\pi^2 A_0^2 \sum_n n}{\sigma_0^2} & \frac{8\pi^2 A_0^2 N}{\sigma_0^2} & 0 & 0 \\ 0 & 0 & \frac{2N}{\sigma_0^2} & 0 \\ 0 & 0 & 0 & \frac{N}{\sigma_0^4} \end{bmatrix}. \tag{19}$$

On the other hand, we have $-\mathbf{A}_{\boldsymbol{\theta}_0} \neq \mathbf{B}_{\boldsymbol{\theta}_0} \neq \mathbf{I}$ in the case of mismatched model.

C. A Lower Bound on Mean Squared Error of Range Estimation

Given the difference vector $\mathbf{r} = \bar{\boldsymbol{\theta}} - \boldsymbol{\theta}_0$ and the misspecified CRB of (11), a lower bound on the MSE for the estimate of the true parameter vector $\bar{\boldsymbol{\theta}}$ under the source nonlinearity is given as

$$\begin{aligned} \mathbf{M}_p(\hat{\boldsymbol{\theta}}(\mathbf{x}), \bar{\boldsymbol{\theta}}) &\triangleq \mathbb{E}_p\left\{(\hat{\boldsymbol{\theta}}(\mathbf{x}) - \bar{\boldsymbol{\theta}})(\hat{\boldsymbol{\theta}}(\mathbf{x}) - \bar{\boldsymbol{\theta}})^T\right\} \\ &= \mathbf{C}_p(\hat{\boldsymbol{\theta}}(\mathbf{x}), \bar{\boldsymbol{\theta}}) + \mathbf{r}\mathbf{r}^T \\ &\succeq \mathbf{A}_{\boldsymbol{\theta}_0}^{-1}\mathbf{B}_{\boldsymbol{\theta}_0}\mathbf{A}_{\boldsymbol{\theta}_0}^{-1} + \mathbf{r}\mathbf{r}^T \end{aligned} \tag{20}$$

It is seen that the MSE of the parameter estimates is bounded by the misspecified CRB and the outer product of the difference vector. For the range estimate, the lower bound is given as

$$\begin{aligned} M_p(\hat{R}(\mathbf{x}), \bar{R}) \succeq &\left(\frac{c}{2\alpha\Delta T}\right)^2 \left[\mathbf{A}_{\boldsymbol{\theta}_0}^{-1}\mathbf{B}_{\boldsymbol{\theta}_0}\mathbf{A}_{\boldsymbol{\theta}_0}^{-1}\right]_{1,1} \\ &+ \left(\frac{c}{2\alpha\Delta T}\right)^2 (f_0 - \bar{f}_0)^2 \end{aligned} \tag{21}$$

where $[\cdot]_{1,1}$ denotes the first diagonal element of the matrix.

IV. Numerical Results

In the following, we consider an automotive FMCW radar at the 79-GHz frequency band. The system parameters are given as: the center frequency $f_c = 79$ GHz, the bandwidth $B = 4$ GHz, the chirp duration $T = 65$ μs, the sampling frequency $f_s = 20$ MHz, and the target is located 10m away from the FMCW transceiver. Fig.2 (a) shows the spectra of ideal (without source nonlinearity) and effectively transmitted (with source nonlinearity) FMCW sources and Fig.2 (b) shows the frequency deviation as a function of sweeping bandwidth. It is seen that the effectively transmitted FMCW waveform has a slightly higher frequency (up to 0.15%) than the ideal frequency at the beginning and lower frequency (up to -2.5%) at the end. The effect of this source nonlinearity on the range spectrum is shown in Fig. 3. In Fig. 3 (a), the spectrum peak is well focused on the true target distance of 10 m, while the peak in Fig. 3 (b) is distorted and slightly shifted to $R_0 = 9.99955$m along with multiple sidelobes.

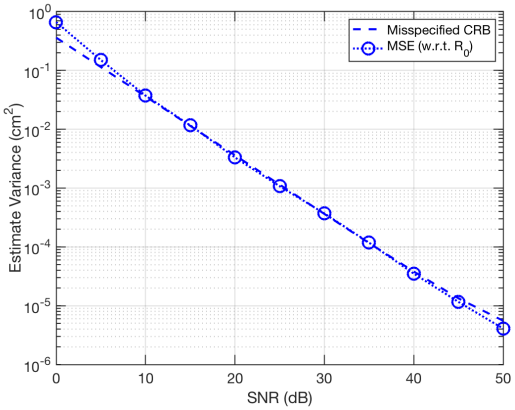

Fig. 4. Misspecified CRB on estimation of pseudo-true range parameter.

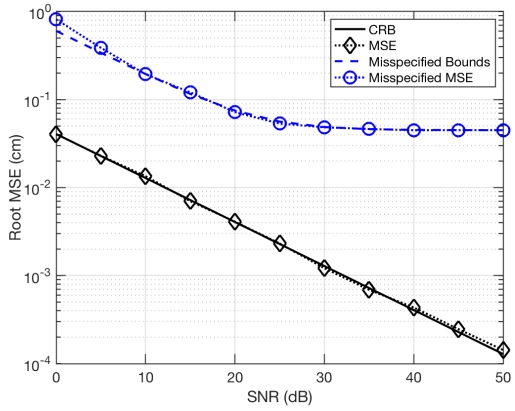

Fig. 5. Lower bounds on estimation of pseudo-true and true range parameters.

Fig. 4 shows the misspecified CRB of (11) using the generalized FIM $\mathbf{A}_{\boldsymbol{\theta}_0}$ and $\mathbf{B}_{\boldsymbol{\theta}_0}$ and compares it with mean-squared errors (MSEs) obtained from Monte-Carlo simulations. It is found that the maximum likelihood range estimator is unbiased with respect to the pseudo-true range parameter $R_0 = 9.99955$m. For a wide range of SNRs, the MSEs (denoted as blue dots) with respect to the pseudo-true range parameter match well with the analytical misspecified CRB (denoted as blue dash line). By taking into account the difference between the pseudo-true and true range parameters, we can compute the lower bound of (21) for the MSEs of range estimates with respect to the true range at 10m. This lower bound (denoted as blue dash line) on the true range estimation is compared with the MSEs

(denoted as blue dots) with respect to the true range parameter in Fig. 5. It is shown that, at high SNRs, the MSEs are dominated by the deterministic deviation between the pseudo-true and true range parameters due to the source nonlinearity, while the noise-induced estimation variance becomes more significant when the SNR is lower. In Fig. 5, the misspecified MSE and lower bound are also compared with the standard CRB (denoted as black solid line) and MSEs (denoted as black diamond) when a perfect FMCW source is used. The performance gap between the blue and black curves characterizes the range accuracy degradation due to the source nonlinearity.

V. Conclusion

In this paper, we provided a theoretical analysis on the effect of FMCW source nonlinearity on range estimation in the presence of source nonlinearity. The theoretical analysis was built on the misspecified CRB framework which first identifies a surrogate (pseudo-true) range parameter in the misspecified signal model and then provides a lower bound on the pseudo-true range parameter estimation. To achieve this goal, we derived two generalized Fisher information matrices which couple the true and misspecified signal models. With the misspecified CRB, we provide a lower bound on the true range estimation as a function of source nonlinearity function, system parameters (bandwidth, sampling frequency, etc.) and SNR.

References

[1] M. Burgos-Garcia, C. Castillo, S. Llorente, J. M. Pardo, and J. C. Crespo, "Digital on-line compensation of errors induced by linear distortion in broadband LFM radars," *Electronics Letters*, vol. 39, no. 1, pp. 116–118, Jan 2003.

[2] A. Meta, P. Hoogeboom, and L. Ligthart, "Range non-linearities correction in FMCW SAR," in *2006 IEEE International Symposium on Geoscience and Remote Sensing*, July 2006, pp. 403–406.

[3] A. Meta, P. Hoogeboom, and L. P. Ligthart, "Signal processing for FMCW SAR," *IEEE Transactions on Geoscience and Remote Sensing*, vol. 45, no. 11, pp. 3519–3532, Nov 2007.

[4] S. O. Piper, "Homodyne FMCW radar range resolution effects with sinusoidal nonlinearities in the frequency sweep," in *Proceedings International Radar Conference*, May 1995, pp. 563–567.

[5] J. Fuchs, K. D. Ward, M. P. Tulin, and R. A. York, "Simple techniques to correct for VCO nonlinearities in short range FMCW radars," in *1996 IEEE MTT-S International Microwave Symposium*, June 1996, pp. 1175–1178.

[6] M. Vossiek, P. Heide, M. Nalezinski, and V. Magori, "Novel FMCW radar system concept with adaptive compensation of phase errors," in *1996 26th European Microwave Conference*, Sept 1996, vol. 1, pp. 135–139.

[7] P. V. Brennan, Y. Huang, M. Ash, and K. Chetty, "Determination of sweep linearity requirements in FMCW radar systems based on simple voltage-controlled oscillator sources," *IEEE Transactions on Aerospace and Electronic Systems*, vol. 47, no. 3, pp. 1594–1604, July 2011.

[8] K. Ramasubramanian and B. Ginsburg, "AWR1243 sensor: Highly integrated 76-81-GHz radar front-end for emerging ADAS applications," in *Texas Instruments, Tech. Rep.*, May 2017, pp. 1–11.

[9] P. Wang, D. Millar, K. Parsons, and P. V. Orlik, "Nonlinearity correction for range estimation in FMCW millimeter-wave automotive radar," in *2018 IEEE MTT-S International Wireless Symposium (IWS)*, May 2018, pp. 1–3.

[10] Y. Liu, D. Goshi, K. Mai, L. Bui, and Y. Shih, "Linearity study of DDS-based W-band FMCW sensor," in *2009 IEEE MTT-S International Microwave Symposium Digest*, June 2009, pp. 1697–1700.

[11] R. J. C. Middleton, D. G. MacFarlane, and D. A. Robertson, "Range autofocus for linearly frequency-modulated continuous wave radar," *IET Radar, Sonar Navigation*, vol. 5, no. 3, pp. 288–295, March 2011.

[12] A. Anghel, G. Vasile, R. Cacoveanu, C. Ioana, and S. Ciochina, "Short-range FMCW X-band radar platform for millimetric displacements measurement," in *2013 IEEE International Geoscience and Remote Sensing Symposium - IGARSS*, July 2013, pp. 1111–1114.

[13] A. Anghel, G. Vasile, R. Cacoveanu, C. Ioana, and S. Ciochina, "FMCW transceiver wideband sweep nonlinearity software correction," in *2013 IEEE Radar Conference (RadarCon13)*, April 2013, pp. 1–5.

[14] A. Anghel, G. Vasile, R. Cacoveanu, C. Ioana, and S. Ciochina, "Short-range wideband FMCW radar for millimetric displacement measurements," *IEEE Transactions on Geoscience and Remote Sensing*, vol. 52, no. 9, pp. 5633–5642, Sept 2014.

[15] M. C. Budge and M. P. Burt, "Range correlation effects in radars," in *The Record of the 1993 IEEE National Radar Conference*, April 1993, pp. 212–216.

[16] S. Scheiblhofer, S. Schuster, and A. Stelzer, "Effects of systematic FMCW radar sweep nonlinearity on bias and variance of target range estimation," in *2006 IEEE MTT-S International Microwave Symposium Digest*, June 2006, pp. 1418–1421.

[17] A. Frischen, J. Hasch, and C. Waldschmidt, "FMCW ramp non-linearity effects and measurement technique for cooperative radar," in *2015 European Radar Conference (EuRAD)*, Sept 2015, pp. 509–512.

[18] S. Ayhan, S. Scherr, A. Bhutani, B. Fischbach, M. Pauli, and T. Zwick, "Impact of frequency ramp nonlinearity, phase noise, and SNR on FMCW radar accuracy," *IEEE Transactions on Microwave Theory and Techniques*, vol. 64, no. 10, pp. 3290–3301, Oct 2016.

[19] C. D. Richmond and L. L. Horowitz, "Parameter bounds on estimation accuracy under model misspecification," *IEEE Transactions on Signal Processing*, vol. 63, no. 9, pp. 2263–2278, May 2015.

[20] S. Fortunati, F. Gini, and M. S. Greco, "The constrained misspecified Cramér-Rao bound," *IEEE Signal Processing Letters*, vol. 23, no. 5, pp. 718–721, May 2016.

[21] S. Fortunati, F. Gini, and M. S. Greco, "The misspecified Cramér-Rao bound and its application to scatter matrix estimation in complex elliptically symmetric distributions," *IEEE Transactions on Signal Processing*, vol. 64, no. 9, pp. 2387–2399, May 2016.

[22] S. Fortunati, F. Gini, M. S. Greco, and C. D. Richmond, "Performance bounds for parameter estimation under misspecified models: Fundamental findings and applications," *IEEE Signal Processing Magazine*, vol. 34, no. 6, pp. 142–157, Nov 2017.

[23] P. Wang, T. Koike-Akino, M. Pajovic, P. V. Orlik, W. Tsujita, and F. Gini, "Misspecified CRB on parameter estimation for a coupled mixture of polynomial phase and sinusoidal FM signals," in *The 44th International Conference on Acoustics, Speech, and Signal Processing (ICASSP 2019)*, May 2019.